**DOI: https://doi.org/10.15276/hait.09.2026.14**
**UDC 004.056:621.391**

# Methodology for land cover change detection in aerial images using a deep convolutional neural network and gradient boosting

**Vita Yu. Kashtan**[1)]
ORCID: https://orcid.org/0000-0002-0395-5895; kashtan.v.yu@nmu.one. Scopus Author ID: 57201902879
**Volodymyr V. Hnatushenko**[1)]
ORCID: https://orcid.org/0000-0003-3140-3788; vvgnat@ukr.net. Scopus Author ID: 6505609275
[1)] Dnipro University of Technology, 19, Dmytro Yavornytskoho Ave. Dnipro, 49005, Ukraine

## ABSTRACT

Tracking surface land cover changes using high-resolution aerial imagery is complicated by the varying spatial resolutions of images, spectral variability, and the presence of optically comparable anthropogenic features. Identifying amber extraction sites is especially difficult because of their fragmented morphology, numerous localized impacts of diverse geometries, and substantial internal heterogeneity. Such factors drastically reduce the precision of traditional pixel-based or threshold-driven methods. **The work aims** to develop a methodology for automated detection of land cover changes using high-resolution aerial photographs, utilizing a deep convolutional neural network to extract high-level spatial texture features and gradient-boosting algorithms to subsequently categorize the observed changes. To achieve this objective, a multi-stage processing pipeline is implemented, including aerial image preprocessing and manual annotation, formation of training and testing datasets, patch-level representation of high-resolution scenes, and spatial aggregation of classification results into continuous thematic maps. **The methodology** explicitly accounts for the spatial context and textural organization of the surface, enabling reliable discrimination between amber mining areas and other visually similar anthropogenic changes. It was implemented in Python, leveraging TensorFlow and Keras for deep learning, along with a gradient boosting framework for final classification. The outputs include a thematic map with three semantic classes: “no change,” “amber mining zones,” and “other changes”, and vectorized contours of disturbed areas, facilitating a spatially explicit representation of changes. Quantitative evaluation using the harmonic mean of precision and recall, the intersection over union coefficient, the root mean square error, the mean absolute error, and the zero-mean normalized cross-correlation demonstrated higher performance for amber mining detection, outperforming standard neural network models. **The practical utility of this work** is its potential to autonomously track human-induced environmental impacts, aid ecological restoration and resource management, and inform management decisions in natural resource governance. The approach offers a scalable solution for high-resolution aerial imagery analysis, advancing intelligent remote sensing technologies and precision environmental monitoring.

**Keywords:** Aerial imagery; land cover change; deep convolutional neural network; gradient boosting; machine learning

***For citation*: Kashtan V. Yu, Hnatushenko V. V. “Methodology for land cover change detection in aerial images using a deep convolutional neural network and gradient boosting”. *Herald of Advanced Information Technolog*. 2026; Vol.9 No.2: 199–211. DOI: https://doi.org/10.15276/hait.09.2026.14**

## INTRODUCTION

Recent breakthroughs in aerospace engineering have facilitated the generation of high-resolution aerial photographs, now available for scientific and applied purposes. Such images, usually in RGB or multispectral band format, provide comprehensive insights into the geometric arrangement of Earth's surface, including shapes, boundaries, and textures. High spatial resolution allows local changes to be detected, which is important for assessing landscape degradation, accurately separating object boundaries, and analysing their colours and textures, thereby increasing the accuracy and the reliability of change detection. Thanks to these properties, high-resolution aerial imagery is widely used in various fields, including cartography, agriculture [1], [2], nature conservation, climatology [3], natural disaster monitoring [4], [5], archaeology, and urban planning [6]. On the other hand, the images' high level of detail creates severe difficulties for manual analysis. Expert interpretation of large amounts of data requires considerable time and effort and is subject to subjective factors and human error. It limits the practical use of such images for large-scale or operational tasks. In this regard, there is a need for automated image processing methods capable of effectively identifying changes on Earth's surface relevant to a specific task and isolating them.

In this work, the term' change detection' (CD) refers to the identification of changes in land cover on a high-resolution aerial photograph by analysing the spatial-spectral properties of the scene in comparison with a reference image. In this research, the reference frame is a high-resolution aerial photo serving as the initial land cover state within the targeted zone during the same seasonal period (September). It is used to form training and test data sets, in particular for manual annotation of amber extraction areas, other anthropogenic changes, and

unchanged areas. A combination of natural and spectral information factors justifies the choice of September as a representative season for analysis. During this period, the active vegetation of the plant cover ceases, reducing its masking effect on surface anthropogenic disturbances, particularly at amber extraction sites. Simultaneously, the absence of snow blankets or seasonal inundations, typically observed during winter and spring, ensures a consistent visual and spectral terrain profile. Furthermore, September offers optimal meteorological conditions (reduced nebulosity), enhancing the clarity of aerospace data and lowering noise interference. Collectively, this enables the acquisition of high-quality imagery for the precise establishment of baseline data and increases consistency in the categorization of terrestrial transitions.

The primary challenge in CD is detecting transformations that are pertinent to a particular objective [7]. The observed changes can be divided into three categories: visible, irrelevant, and relevant [8]. Visible changes arise due to changes in shooting conditions (lighting, atmospheric conditions, sensor settings) and do not reflect the actual transformations of objects. Fundamental changes occurring in objects are divided into relevant and irrelevant, and their classification depends on the specifics of the task. For example, snow cover is irrelevant for urban planning but important for assessing glacier conditions; vegetation moisture levels do not affect cartography but are essential for crop monitoring. Anthropogenic changes may be important for monitoring activities, but may not affect archaeological research.

Thus, the combination of high-resolution aerial imagery and automated analysis methods enables accurate and efficient detection of changes on Earth's surface, which is key to rapid, large-scale monitoring of landscape degradation and anthropogenic impacts.

## RELATED WORKS

The task of detecting changes in images of Earth's surface is a classic area of research in remote sensing and computer vision and has been actively developing for several decades. Existing approaches to change detection can be broadly grouped into five classes: direct image comparison methods, statistical methods, spatial-spectral transformation methods, machine learning (ML) methods, and deep learning methods.

Pixel-based comparison techniques, frequently termed algebraic approaches, rely on computing pixel-level discrepancies or evaluating spectral profiles between multi-temporal datasets. Typically, these procedures involve two phases: initially, a difference map is generated (using techniques such as subtraction, ratioing, or regression analysis), followed by the application of a threshold to produce a binary classification. This category encompasses image differencing, regression, correlation, and Change Vector Analysis [9, 10]. A key benefit of these strategies is their straightforward execution and low computational complexity. However, their performance is heavily contingent upon the chosen threshold, which dictates the system's sensitivity. Consequently, these methods often necessitate manual tuning for specific datasets or research objectives.

Statistical methods are based on the analysis of pixel-value distributions and their statistical characteristics for both the entire image and its individual fragments. Changes are identified as statistically significant deviations between images from different time slices. Such methods are most often used to analyse hyperspectral data [11] and images obtained using synthetic aperture radar [12], since these types of data are usually characterised by fewer visible changes due to shooting conditions than multispectral images with high spatial resolution.

Methods based on spatial-spectral transformations involve preliminary transformations of input images to enhance informative changes and suppress unchanging or random variations. This class includes principal component analysis [13], multidimensional change detection [14], Gram-Schmidt transformation, and the 'hat with tassels' method. Utilizing these transformations enables researchers to isolate the most significant data components. However, these methods, like direct comparison methods, often require additional thresholding to produce a change map, and deciphering the outcomes within the modified feature space can be complex.

A variety of predictive architectures have been employed to identify modifications, notably support vector machines [15], [16], random forests [17], [18], decision trees, multi-level methods [19], alongside graphical probability-based frameworks, including Markov Random Fields [20] and their conditional counterparts. The use of such models enabled consideration of statistical and spatial dependencies between pixels, thereby ensuring sufficiently high change-detection accuracy in some cases. Despite successful results for individual datasets, most classical machine learning methods are characterised by limited generalisation ability.


ISSN 2663-0176 (Print)
ISSN 2663-7731 (Online)

Their effectiveness depends heavily on feature selection, classifier type, model parameters, and threshold settings, which complicates transferring such approaches to other scenes or shooting conditions. In addition, the pixel-by-pixel nature of the analysis limits these methods' ability to fully capture the intricate spatial dependencies, which remains a crucial requirement for interpreting high-resolution aerial images.

A separate class of modern approaches comprises deep learning-based change-detection methods. Unlike these approaches, deep learning methods do not eliminate the need for handcrafted features, enabling the unified learning of spatiotemporal and radiometric representations directly from data. Deep convolutional neural networks (CNNs) can automatically form multi-level, hierarchical feature representations, enabling effective modelling of complex interdependencies between geographic and spectral variables in remote sensing data [21]. The paper [22] investigates land cover classification and change detection using Sentinel-2 data with FCN and a multi-temporal FCN-LSTM. It shows that multi-temporal models are more effective than mono-temporal ones. The approach is designed for medium-scale spatial data and fails to capture localized, human-induced. The paper [23] proposes an intelligent Sentinel-2 data processing technology that combines geometric and radiometric corrections, the Dark Object Subtraction algorithm, a hybrid CNN architecture (CNN + EfficientNet-Edge), and a change-detection method based on symmetric pixel differences, ensuring high accuracy and efficiency in land-cover change analysis. It is due to DCNNs' ability to form nonlinear, multi-level feature representations, which ensure effective modelling of complex spatial-spectral dependencies.

Thus, an evaluation of contemporary change-monitoring strategies detection indicates a gradual transition from classical pixel-by-pixel and threshold methods to intelligent models capable of automatically forming informative spatial-spectral representations and providing more stable, reliable change detection in high-resolution images. A major drawback of conventional change-tracking techniques is their high sensitivity to visible changes caused by shooting conditions, atmospheric influences, or sensor noise. In contrast, interpret individual pixels by evaluating their neighborhood context and using high-level features for decision-making, thereby significantly reducing the number of false positives. In addition, unlike traditional approaches based on spectral indices or predefined band combinations, deep neural networks can utilize all available spectral information without the need for expert feature selection. The model automatically determines the weight and contribution of each spectral band during training.

The above limitations of classical approaches justify further research into developing deep learning architectures for identifying changes in high-resolution aerial photographs.

## RESEARCH AIM AND OBJECTIVES

The work aims to develop a methodology for automated detection of land cover changes using high-resolution aerial photographs, based on the Residual Neural Network with 50 layers (ResNet50) convolutional neural network to extract high-level spatial texture features and gradient-boosting algorithms for further classification of the detected changes. The proposed methodology not only identifies land cover changes but also generates vectorised contours of disturbed areas, particularly areas of illegal amber mining.

To achieve these aims, the following tasks are to be performed:

– to analyse existing methods of mapping land cover and landscape changes based on high-resolution aerial photographs;

– to pre-process and annotate high-resolution images to identify three thematic classes: ‘no change’, ‘amber mining areas’, and ‘other anthropogenic changes’;

– to adapt the ResNet50 architecture to convert the spectral and textural characteristics of the image into a high-dimensional spatial descriptor;

– to integrate the eXtreme Gradient Boosting (XGBoost) to classify the extracted features;

– to optimise the loss function to minimise errors when working with unbalanced data;

– to develop a structural diagram of the methodology for intelligent mapping of land cover changes using high spatial resolution aerial photographs.

## RESEARCH METHODOLOGY

The proposed methodology for automated detection and mapping of land cover changes using high-resolution aerial imagery is presented in Fig.1. The proposed method is based on a combination of deep convolutional analysis of spatial-textural features with ML-based classifiers to categorize identified transitions and the subsequent spatial reconciliation of results to form vectorised contours of disturbed areas.

The methodology includes five consecutive steps:

1) to prepare the input data and form a reference set;

2) to extract high-level features using a convolutional neural network;

3) to train a change classifier;

4) to spatial mapping of results;

5) to create vectorised contours of changes in the Earth's surface on primary aerial photographs.

The process begins with the acquisition of high-resolution aerospace imagery. High-resolution aerial photographs measuring 1533×945×3 pixels in the visible spectral range (RGB) are used as input data. Such images are characterised by great spatial detail, which allows small-scale anthropogenic changes in land cover to be recorded. To ensure stable algorithm operation, pre-processing [24] of the raw data is performed to reduce the influence of factors unrelated to actual land cover changes, including channel brightness normalisation, histogram equalisation to increase contrast, and noise reduction. This step allows us to reduce the number of so-called visible changes arising from shooting conditions rather than from transformations of objects on Earth's surface.

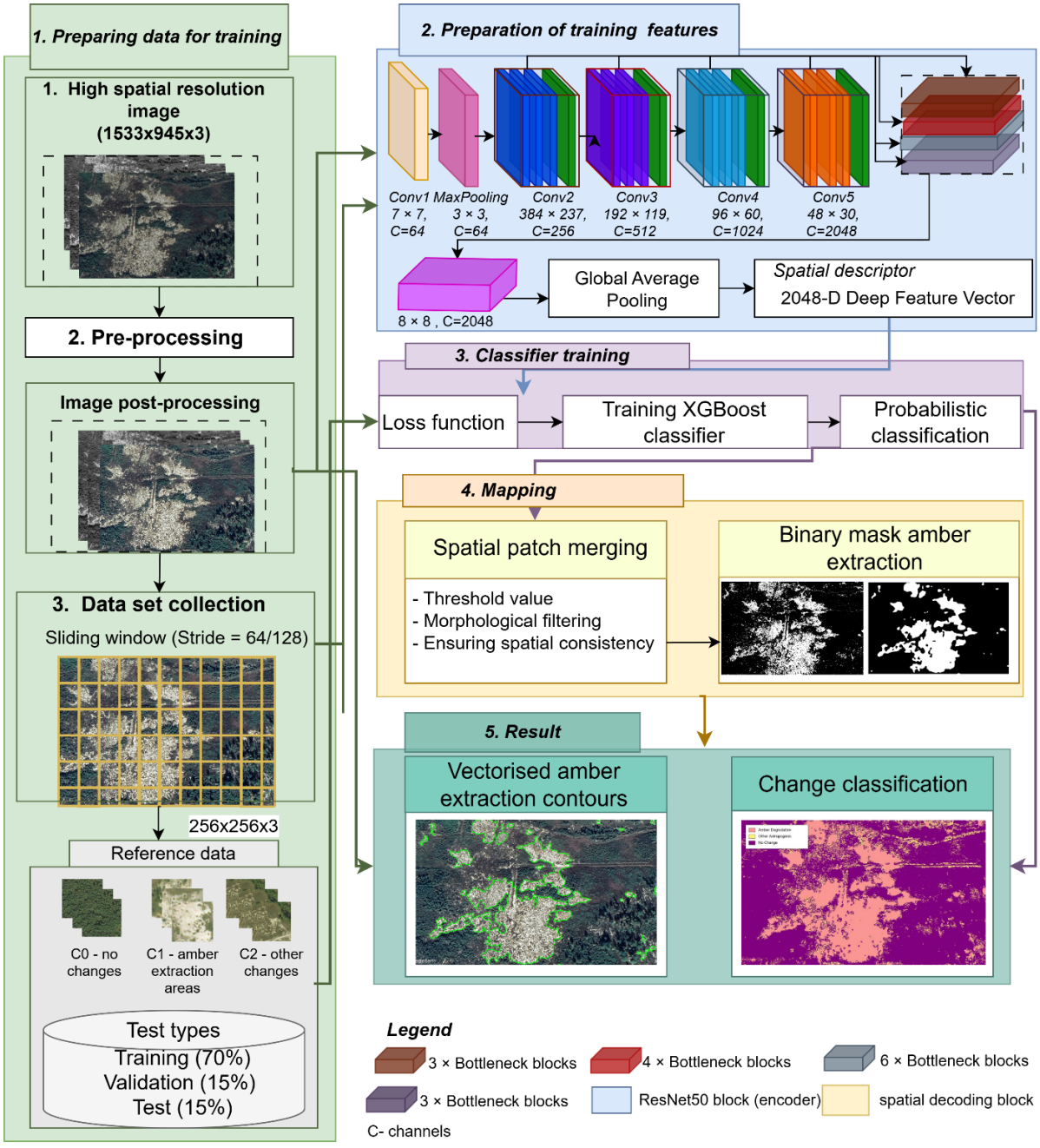


*Fig. 1.* **Conceptual schema of the developed methodological workflow**
***Source*: prepared by the authors**

To ensure the effective optimization of deep learning and machine learning architectures while simultaneously enhancing the reliability of change-detection outcomes, a pivotal phase of the methodology involves developing a representative training dataset focused on monitoring illegal amber extraction in the Rivne and Zhytomyr regions of Ukraine. The integrity and organizational structure of this data collection directly determine the model's ability to differentiate between substantive land-cover transitions and superficial noise or variations arising from specific imaging conditions. Given that high-resolution aerial photographs exceed the capacity of convolutional neural networks for direct processing, a patch-based learning strategy is implemented. The original imagery is partitioned into sub-frames of 256×256×3 pixels using a sliding window with a step of 64 or 128 pixels. The resulting dataset is strictly balanced and consists of 2,961 unique image fragments, with exactly 987 samples for each of the three defined classes: $C0$ – areas without changes; $C1$ – amber extraction areas; $C2$ – other changes (anthropogenic objects (roads, clearings) not related to extraction). The training data set was annotated by expert interpretation of high-resolution aerial photographs, accounting for the characteristic morphological, spectral, and textural features of anthropogenically disturbed areas. Particular focus was placed on establishing the amber extraction reference class, as this specific category of land transformation poses significant automated recognition challenges and is frequently misinterpreted as other types of land-cover degradation. Amber extraction areas are characterised by a specific spectral-textural response, which was formalised within this study as a set of diagnostic features (Fig. 2). These features include: intense light sandy-clay spots of bare soil that contrast sharply with the surrounding vegetation in RGB images; the presence of numerous micro-water bodies of chaotic shape (flooded pits), which appear as dark spots with characteristic spectral absorption, in particular in the near-infrared range; a radially chaotic structure of surface disturbances, forming a so-called 'lunar landscape' and lacking the geometric orderliness characteristic of legal quarries or agricultural land; sharp breaks in the forest canopy and linear traces of anthropogenic impact, in particular temporary roads for motor pumps, which can be traced within forest areas. Using these diagnostic markers, manual boundary delineation of amber extraction sites was conducted, enabling the production of binary masks for class *C1*. This approach to annotation allows us to move from subjective visual recognition to a formalised description of the class of land-use changes, which is essential for subsequent training of deep learning architectures and for ensuring the reproducibility of experimental results. The resulting dataset is partitioned into training (70 %), validation (15 %), and testing (15 %) subsets.

For the automated extraction of high-level spatial-textural features during the second methodological step, we used a ResNet50 convolutional neural network, a class of deep residual learning frameworks [25]. A defining characteristic of ResNet is the integration of residual connections; these allow robust optimization of extremely deep architectures by preventing gradient degradation during backpropagation.

Mathematically, the residual function is described by the relationship (1) [25]:

$$y = F(x, W) + x, \quad (1)$$

where $x$ is the input tensor, $F$ is a nonlinear transformation implemented by a sequence of convolutions, and $W$ is a set of weights.

Based on the analysis of existing deep learning approaches for remote sensing, ResNet50 was selected as the core feature encoder for this study. While simpler architectures often struggle with the vanishing gradient problem during deep feature extraction, ResNet50 utilizes residual learning blocks to enable the effective training of high-level hierarchical representations. It is particularly critical for identifying the complex “lunar landscape” of amber extraction sites (Class $C1$), where subtle textural and morphological nuances distinguish amber mining from other anthropogenic disturbances.

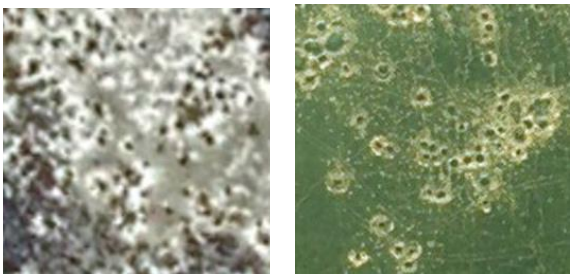

*Fig. 2*. **Example of amber extraction area data set**
***Source*: prepared by the authors**

As shown in Fig. 1, ResNet50 consists of the following main stages: Conv1 – initial 7×7 convolution with a stride of 2 and 64 filters, which provides initial extraction of low-level features; MaxPooling – reduction of spatial size for the purpose of aggregating local patterns; Conv2_x – Conv5_x – four consecutive blocks with residual

bottleneck layers (3, 4, 6 and 3 blocks, respectively), in which the number of channels gradually increases from 256 to 2048. Each bottleneck block contains three convolutional layers with 1×1, 3×3, and 1×1 kernels, reducing computational complexity without sacrificing feature representativeness.

At the output of the convolutional part, Global Average Pooling is applied, which converts a multidimensional tensor into a feature vector of dimension 2048 according to the formula (2):

$$f = \frac{1}{H \cdot W} \sum_{i=1}^{H} \sum_{j=1}^{W} F_{i,j}, \quad (2)$$

where $F_{i,j}$ are the activation values at position ($i$, $j$). The resulting vector describes the spectral-textural characteristics of each image fragment.

In the third step, the XGBoost gradient boosting algorithm [26] is used to classify deep feature vectors, demonstrating high noise tolerance and effective performance on unbalanced data.

The model is trained by minimising the regularised loss function as defined in equation (3) [26]:

$$\mathcal{L}^{(t)} = \sum_{i=1}^{n} l\left(y_i, \hat{y}_i^{(t-1)} + f_t(x_i)\right) + \Omega(f_t), \quad (3)$$

where $l(\cdot)$ is the loss function, and $\Omega(f_t)$ is the regularisation term that controls the complexity of the model.

For effective optimisation, the second-order approximation of the loss function is used by formula (4) [26]:

$$\mathcal{L}^{(t)} \approx \sum_{i=1}^{n} \left[g_i, f_t(x_i) + \frac{1}{2} h_i f_t^2(x_i)\right] + \Omega(f_t), \quad (4)$$

where $g_i$ is the first derivative of the loss function, respectively; hi is the second derivative of the loss function, respectively.

The quality of the spatial breakdown of features in a decision tree is assessed using the loss-function-increment criterion, which allows the effective selection of informative spatial features for mapping tasks via formula (5) [26]:

$$\mathcal{L}_{split} = \frac{1}{2}\left[\frac{\left(\sum_{i \in I_L} g_i\right)^2}{\sum_{i \in I_L} h_i + \lambda} + \frac{\left(\sum_{i \in I_R} g_i\right)^2}{\sum_{i \in I_R} h_i + \lambda} - \frac{\left(\sum_{i \in I_I} g_i\right)^2}{\sum_{i \in I_I} h_i + \lambda}\right] - \gamma, \quad (5)$$

where $I_L$ and $I_R$ are represented by the subsets of sample indices assigned to the left and right child nodes after the split, respectively; $I = I_L \cup I_R$ is the complete set of sample indices in the current parent node; $\lambda$ is the $L_2$ regularization parameter on leaf weights; $\gamma$ is the complexity cost (minimum loss reduction required) to perform a split.

The result of this stage is a probabilistic assessment of each fragment's belonging to the corresponding class of changes.

In the fourth stage, the classification results are projected back into the original image space. Since the model outputs a probability $P\epsilon$ [0, 1] for each patch belonging to class $C_1$, an optimal classification threshold $T$ is applied to generate the binary mask. In this study, the threshold was determined using Precision-Recall curve analysis, selecting $T = 0.5$ to balance the detection of small-scale extraction pits while minimizing false positives from similar spectral-textural features in class $C_2$. Based on this, a binary mask of amber extraction areas is formed (Fig. 3).

The fifth stage involves vectorizing the binary masks and constructing thematic maps that delineate the contours of disturbed areas and represent the classification of land cover changes. To ensure spatial consistency, a morphological closing operation with a 3 × 3 pixel structuring element is applied to the binary mask. This operation fills small internal gaps within detection clusters and smooths the boundaries of disturbed regions. The boundaries of the refined binary regions are extracted using the Suzuki-Abe contour tracing algorithm, which establishes a hierarchical relationship between external and internal contours (holes). To ensure compatibility with GIS environments, the extracted vertices are simplified using the Douglas-Peucker algorithm. A tolerance threshold is applied to preserve high geometric fidelity to the original high-resolution imagery while removing redundant nodes. The resulting polygons are attributed with thematic information (class *C1*) and reprojected into the original geographic coordinate system, enabling the generation of final thematic maps.

*Fig. 3.* **Example of a binary mask for an amber extraction area**
***Source*: prepared by the authors**

## EXPERIMENTS

The proposed methodology was implemented and tested in Python using the TensorFlow and Keras libraries to train the ResNet50 convolutional neural network, and the XGBoost library to build a gradient-boosted classifier. Image pre-processing


ISSN 2663-0176 (Print)
ISSN 2663-7731 (Online)

and analysis were performed using the NumPy, OpenCV, and GDAL libraries.

Computational experiments were performed on a personal computer with an Intel Core i7 processor, 32 GB of RAM, and an NVIDIA graphics accelerator (CUDA-compatible), which enabled practical model training and stable loss-function convergence during long training (up to 300 epochs).

The study was conducted for the territory of the village of Shebedykha in the Olevsk district of the Zhytomyr region, which is characterised by a significant concentration of anthropogenic disturbances caused by amber mining (Fig. 4). The analysis used a high-resolution digital aerial photograph from 2020, which provides a detailed representation of small-scale changes in land cover and allows the identification of localised areas of landscape degradation.

*Fig. 4*. **High spatial resolution digital test aerial photograph after preliminary processing**
***Source*: prepared by [27]**

The proposed methodology included a deep learning stage comprising a ResNet50 encoder and an XGBoost classifier. Training was conducted over 300 epochs to achieve stable convergence and minimise the loss function. Evaluation of the accuracy trends alongside the loss function stabilization for both training and cross-validation sets accompanied the model's training. Fig. 5 illustrates the evolution of categorical classification performance over training duration. According to the visualized data (Fig. 5), even at the initial stages of training (epochs 30-50), accuracy increases rapidly on both the training and validation sets, indicating the model's effective assimilation of basic spatial-spectral features. Further training is characterised by a gradual convergence of the training and validation accuracy curves, with the maximum validation accuracy reaching 0.977, indicating the high generalisation ability of the proposed methodology. The lack of a sharp difference between the training and validation accuracy curves indicates minimal overfitting, even after prolonged training (up to 300 epochs).

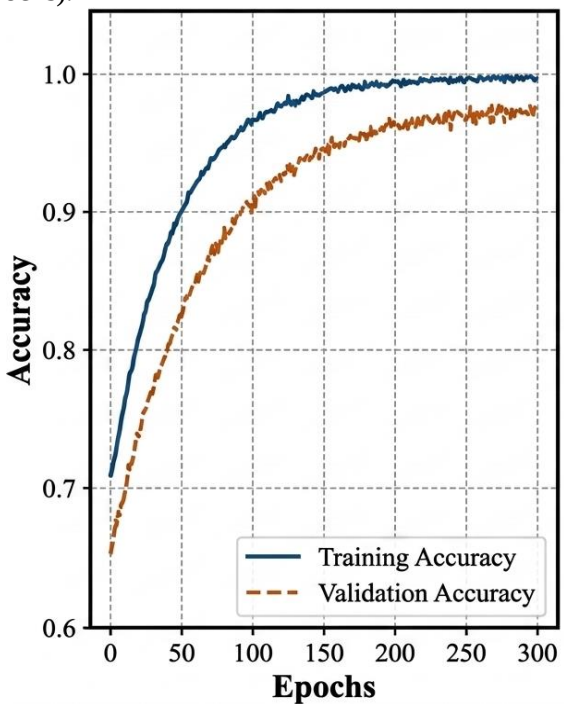


*Fig. 5*. **Accuracy indicators of the proposed model implemented based on the ResNet50 architecture in combination with XGBoost**
***Source*: prepared by the authors**

Fig. 6 shows the convergence behavior of the loss function, quantified via the Root-Mean-Square Error (RMSE) metric. With the progression of training epochs, the loss value exhibits a monotonic decline for both the training and validation datasets. The initial sharp decrease in RMSE indicates rapid optimisation of the model parameters. At the same time, in the later stages of training, the curve becomes flat, indicating that a stable minimum has been reached. The final RMSE on the validation sample is 0.084, validating the high precision of the numerical approximation and the suitability of the chosen objective function for identifying human-induced land-cover transformations.

To assess the spatial accuracy of land cover change detection, a set of statistical error indicators was calculated. The final values of the metrics are presented in Table 1.

To ensure an unbiased evaluation of the developed approach for the autonomous mapping of land surface transitions, a robust quantitative assessment of the classification outcomes was executed on a high-resolution test aerial photograph. The assessment was carried out by comparing the results of automatic classification with reference markings derived from expert visual interpretation. Considering the multi-class complexity of the objective and the distinct spatial characteristics of

land-cover modifications, a suite of standardized performance indicators was utilized to thoroughly assess both the per-class recognition accuracy and the general model efficiency. The following statistical parameters were computed for each class: Precision, Recall, F1-Score, and Intersection over union (IoU) in Table 2 [28].

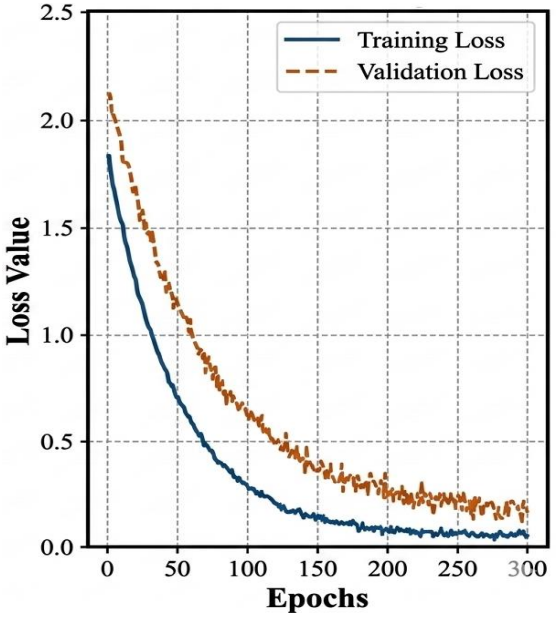


*Fig. 6*. **RMSE metric values during training of the proposed model implemented based on the ResNet50 architecture in combination with XGBoost**

***Source*: compiled by the authors**

*Table 1.* **Quantitative indicators of error metrics and structural similarity with the reference image**

| Metric | Value |
|---|---|
| RMSE | 0.084 |
| MAE | 0.052 |
| cRel | 0.068 |
| ZNCC | 0.892 |

***Source*: compiled by the authors**

*Table 2.* **Values of land cover classification accuracy metrics**

| Object class | Precision | Recall | F1-Score | IoU |
|---|---|---|---|---|
| Amber extraction | 0.94 | 0.91 | 0.92 | 0.86 |
| Other Changes | 0.88 | 0.85 | 0.86 | 0.76 |
| No Change | 0.97 | 0.98 | 0.97 | 0.94 |
| Weighted Avg | | | | |
| - | 0.93 | 0.91 | 0.92 | 0.85 |

***Source*: compiled by the authors**

To evaluate the effectiveness of the proposed methodology, a comparative analysis was conducted with common deep learning and classical segmentation approaches widely used for analysing high-resolution aerial photographs. The results of the comparison are presented in Table 3.

*Table 3.* **Comparative characteristics of architectures in detecting amber mining areas**

| Architecture | Output type | Overall Accuracy | Mean IoU | F1-Score (Amber) | Number of parameters |
|---|---|---|---|---|---|
| VGG16 | Patch classification | 0.821 | 0.714 | 0.795 | ~138 million |
| ResNet50 (Standard) | Patch classification | 0.884 | 0.796 | 0.872 | ~25 million |
| U-Net | Pixel-by-pixel segmentation | 0.864 | 0.782 | 0.841 | ~31 million |
| Proposed (ResNet50 + XGBoost) | Classified change map with vectorised contours | 0.914 | 0.856 | 0.923 | ~25 million |

***Source*: compiled by the authors**

## RESULTS AND DISCUSSIONS

Fig. 7 shows the result of applying the proposed methodology for mapping land cover changes with highlighted vectorised contours of amber mining areas.

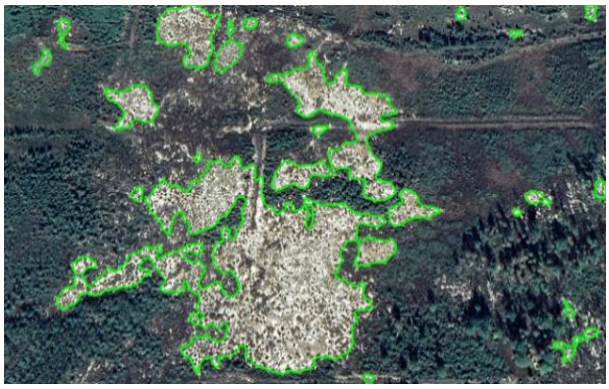

*Fig. 7*. **High spatial resolution digital test aerial photograph highlighting of amber extraction contours using the proposed methodology**

***Source*: prepared by the authors**

The contours obtained reflect the actual boundaries of technogenically disturbed areas and were derived directly from the analysis of spectral-textural image features and subsequent


ISSN 2663-0176 (Print)
ISSN 2663-7731 (Online)

classification. The selected areas are characterised by a complex, irregular shape and high spatial heterogeneity, resulting from the local, uncontrolled, and fragmentary nature of hydromechanical extraction. The contours of the extraction areas spatially correspond to the visually identified signs of land cover degradation in the original image, including areas of exposed light-coloured soil, numerous small water-filled depressions, and sharp boundaries of forest cover disturbance.

The resulting map of changes is organised into three thematic classes: ‘amber extraction areas,’ ‘other changes,’ and ‘unchanged territories’ (Fig.8).

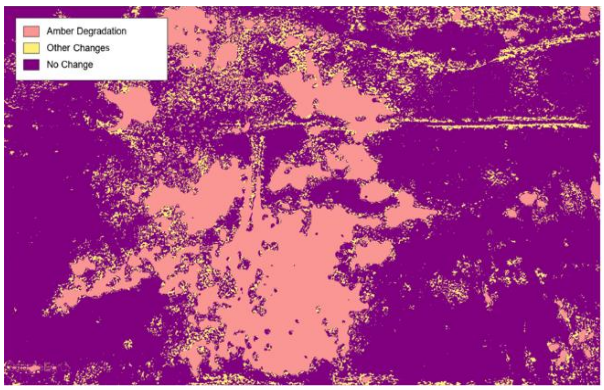


*Fig. 8*. **Maps of land cover changes on aerial photographs with high spatial resolution using the proposed methodology**
***Source*: prepared by the authors**

The delineated boundaries of amber mining zones exhibit a high degree of morphological complexity, including a complex configuration, with numerous local protrusions and depressions, a lack of geometric uniformity, and substantial fluctuations in the spatial extent of discrete sites. Visual analysis of the results shows that the model correctly identifies both large, contiguous areas of degraded territory and small, isolated mining sites within forest areas. The proposed methodology must allow for distinguishing amber extraction areas from collateral anthropogenic transformations (e.g., logging tracks, forest openings, or reclaimed lands). While these features share spectral similarities, they diverge significantly in their spatial configuration and textural structure. The results confirm that combining deep feature extraction with the ResNet50 architecture and subsequent classification with the gradient boosting algorithm achieves high spatial consistency and reduces the number of false positives characteristic of classical pixel-by-pixel methods. The generation of vectorized polygons for the identified change areas enables their immediate application in thematic cartography, land degradation surveillance, and managerial decision-making.

Statistical evaluation of the metrics presented in Table 1 reveals that the Root-Mean-Square Error (0.084) and Mean Absolute Error (0.052) fall within acceptable thresholds for high-resolution aerospace images, guaranteeing high accuracy in the localisation of pits. The relative error indicator cRel (0.068) provides validation that the cumulative area of identified landscape degradation zones in the Shebedykha tract aligns with ground-truth data, achieving a precision exceeding 93 %. A robust ZNCC correlation value (0.892) underscores the significant structural alignment between the model's predictive output and the reference annotations.

In Table 2 for the 'Amber extraction' class, high values of Precision = 0.94 and Recall = 0.91 were obtained, which indicates the ability of the methodology to effectively separate areas of technologically disturbed soil from background types of land cover. The F1-Score = 0.92 confirms the model's balance between accuracy and completeness of detection, while IoU = 0.86 indicates a high spatial correspondence between automatically generated contours and the reference boundaries of extraction areas.

Regarding the 'Other changes' class, slightly lower metric values were recorded (F1 = 0.86, IoU = 0.76), which is attributed to the inherent spectral and textural diversity within this class, encompassing features with varied origins and levels of degradation. Nevertheless, the indicators obtained demonstrate the model's stable ability to maintain generalizability across diverse anthropogenic impacts.

The 'No change' class is characterised by the highest accuracy values (Precision = 0.97, Recall = 0.98, IoU = 0.94), which is due to the relative spectral homogeneity and spatial integrity of the natural forest cover. The weighted average of the metrics demonstrates the overall effectiveness of the proposed methodology: F1-Score = 0.92 and IoU = 0.85, confirming its suitability for automated detection and mapping of land cover changes in high-resolution aerial photographs.

In Table 3, the basic models used are the VGG16 architecture, adapted for patch classification, and ResNet50 in its standard configuration, without additional decision-making modules.

The U-Net model, which implements a pixel-by-pixel semantic segmentation approach and is often used for land cover change detection tasks, is considered separately. The methodology proposed in this work is based on a combination of the ResNet50

convolutional neural network for extracting high-level spectral-textural features and the XGBoost gradient boosting algorithm for further classification of spatial descriptors.

The VGG16 architecture achieves the lowest Accuracy (Overall Accuracy = 0.821, Mean IoU = 0.714), due to a large number of parameters (~138 million) and limited generalisation to complex spectral-textural patterns characteristic of areas of illegal amber mining.

The use of ResNet50 in standard patch classification mode provides a significant quality improvement (F1-Score = 0.872) due to residual connections and more efficient feature extraction with significantly fewer parameters (~25 million). However, this approach does not fully account for the spatial context of adjacent areas.

The U-Net model, focused on pixel-by-pixel segmentation, achieves stable results (Mean IoU = 0.782). However, in fragmented, spatially heterogeneous areas of degradation, its effectiveness is reduced due to its sensitivity to noise and difficulty in clearly separating class boundaries.

The highest values were obtained for the proposed methodology (ResNet50 + XGBoost) Overall Accuracy = 0.914, Mean IoU = 0.856, F1-Score for the class ‘Amber extraction’ = 0.923. It indicates that using an ensemble decision-making algorithm on top of deep features enables effective separation of relevant changes from background and random variations, as well as the formation of spatially consistent contours of disturbed areas.

An important aspect of the proposed methodology is its potential to generalize across different geographical regions and environmental conditions. The model relies not only on spectral characteristics but also on spatial–textural descriptors extracted by the ResNet50 architecture. These descriptors reflect morphological patterns typical of amber mining sites, such as irregular pit clusters, fragmented disturbed surfaces, and characteristic spatial heterogeneity. Since such structural features are largely independent of specific geographic location, the methodology can be transferred to other regions with similar manifestations of illegal amber extraction, provided that representative training samples are available.

Another factor affecting the model's applicability is seasonal variability. Seasonal changes in vegetation phenology may influence spectral responses in optical imagery, potentially affecting the separability between disturbed soils and surrounding vegetation cover. However, the use of deep convolutional features that integrate multi-scale spatial context reduces the dependence on purely spectral differences. As a result, the model demonstrates increased robustness to moderate seasonal variations, although additional seasonal samples in the training dataset may further enhance stability.

The methodology's sensitivity to variations in spatial resolution should also be considered. The model was trained using high-resolution aerial imagery, in which the spatial structure of extraction pits and disturbed areas is clearly visible. When applied to data with lower spatial resolution, the visibility of fine-scale morphological details decreases, potentially reducing detection accuracy for small mining sites. Nevertheless, the patch-based processing strategy and feature aggregation within the ResNet50 architecture allow the method to retain its effectiveness for medium-resolution imagery, particularly for larger disturbed areas.

## CONCLUSIONS

This study introduces a novel methodology for detecting land cover changes using high-resolution aerial photographs, focused on identifying anthropogenic disturbances caused by amber mining. The methodology is based on a combination of the ResNet50 deep convolutional neural network for extracting high-level spatial-spectral features and the XGBoost gradient boosting algorithm for their further semantic classification. It has been shown that deep hierarchical features enable effective separation of fundamental land cover changes from visible variations caused by shooting conditions, atmospheric influences, and sensor noise, which significantly limit the accuracy of classical threshold and per-pixel methods. Unlike standard techniques, the introduced approach integrates the inherent spatial and textural complexities of the terrain, which are essential for processing high-resolution aerial imagery. Implementation of this methodology yielded a map of land cover changes was created according to three semantic classes (“amber extraction areas”, “no changes”, “other changes”), alongside a classified map of changes with vectorised contours of amber extraction areas, suitable for further geoinformation analysis and assessment of landscape degradation areas. Vectorisation of the boundaries of disturbed areas increases the practical value of the results and enables their integration into environmental monitoring and spatial planning systems. A quantitative assessment of effectiveness confirmed the high accuracy of the proposed approach. For the ‘amber extraction areas’ class, F1-score values of 0.92 and IoU values of 0.86 were achieved, which exceeds the performance of classical patch classification and pixel-by-pixel segmentation architectures. A comparative analysis with VGG16,


ISSN 2663-0176 (Print)
ISSN 2663-7731 (Online)

standard ResNet50, and U-Net models showed that the proposed combination of ResNet50 + XGBoost provides an optimal balance between accuracy, generalisation ability, and the number of model parameters.

The authors used Grammarly to check the grammar and spelling. After using this tool, the authors reviewed and edited the content as needed and take full responsibility for the publication's content.

## ACKNOWLEDGEMENTS

This research is carried out as part of the scientific project no.0126U000995 "Intelligent technologies for analyzing spatiotemporal changes in aerospace imagery to support decision-making under conditions of armed aggression" funded by the Ministry of Education and Science of Ukraine at the expense of the state budget.

## REFERENCES

1. Shitharth, S., Manoharan, H., Alshareef, A. M., Yafoz, A., Alkhiri, H. & Mirza, O. M. "Hyper spectral image classifications for monitoring harvests in agriculture using fly optimization algorithm". *Computers and Electrical Engineering*. 2022; 103: 108400, https://www.scopus.com/pages/publications/85138783303.
DOI: https://doi.org/10.1016/j.compeleceng.2022.108400.

2. Kashtan, V. Yu., Hnatushenko, V. V., Laktionov, I. S. & Diachenko, H. H. "Intelligent Sentinel satellite image processing technology for land cover mapping". *Naukovyi Visnyk Natsionalnoho Hirnychoho Universytetu*. 2024; (5): 143–150, https://www.scopus.com/pages/publications/85209234953. DOI: https://doi.org/10.33271/nvngu/2024-5/143.

3. Zhang, E., Liu, L., Huang, L. & Ng, K. S. "An automated, generalized, deep-learning-based method for delineating the calving fronts of Greenland glaciers from multi-sensor remote sensing imagery". *Remote Sens. Environ.* 2021; 254: 112265, https://www.scopus.com/pages/publications/85098455848. DOI: https://doi.org/10.1016/j.rse.2020.112265.

4. Kashtan, V. Yu. & Hnatushenko, V. V. "Deep learning technology for automatic burned area extraction using satellite high spatial resolution images". *Lecture Notes in Computational Intelligence and Decision Making, Springer, Cham*. 2023; 1246: 664–685, https://www.scopus.com/pages/publications/85138742653. DOI: https://doi.org/10.1007/978-3-031-16203-9_37.

5. Román, A., Tovar-Sánchez, A., Larrad, M., et al. "UAV imagery in natural disasters: Real-time damage assessment of flash flooding events". *Ecological Informatics*. 2025; 91: 103433, https://www.scopus.com/pages/publications/105016219627.
DOI: https://doi.org/10.1016/j.ecoinf.2025.103433.

6. Kashtan, V. Yu. & Hnatushenko, V. V. "Automated building damage detection on digital imagery using machine learning". *Naukovyi Visnyk Natsionalnoho Hirnychoho Universytetu*. 2023; (6): 134–140, https://www.scopus.com/pages/publications/85182447348. DOI: https://doi.org/10.33271/nvngu/2023-6/134.

7. Cheng, G., Huang, Y., Li, X., Lyu, S., Xu, Z., Zhao, H., Zhao, Q. & Xiang, S. "Change detection methods for remote sensing in the last decade: A comprehensive review". *Remote Sens.* 2024; 16 (13): 2355. DOI: https://doi.org/10.3390/rs16132355.

8. Parelius, E. J. "A review of deep-learning methods for change detection in multispectral remote sensing images". *Remote Sens.* 2023; 15 (8): 2092, https://www.scopus.com/pages/publications/85156193999. DOI: https://doi.org/10.3390/rs15082092.

9. Yao, Y., Jiang, Y., Sun, Z., Li, L., Chen, D., Xiong, K., Dong, A., Cheng, T., Zhang, H., Liang, X., Guan, Q. "Applicability and sensitivity analysis of vector cellular automata model for land cover change". *Computers, Environment and Urban Systems.* 2024; 109: 102090, https://www.scopus.com/pages/publications/85185407256.
DOI: https://doi.org/10.1016/j.compenvurbsys.2024.102090.

10. Al-Khaqani, E. & Hamid, H. "Monitoring land cover dynamics utilizing a change vector analysis approach: a case study of al Najaf Province, Iraq". *Kuwait Journal of Science*. 2022, https://www.scopus.com/pages/publications/85164351545. DOI: https://doi.org/10.48129/kjs.16391.

11. Lv, Z., Zhang, M., Sun, W., Lei, T., Benediktsson, J. A. & Liu, T. "Land cover change detection with hyperspectral remote sensing images: A survey". *Information Fusion*. 2025; 123: 103257, https://www.scopus.com/pages/publications/105004560874. DOI: https://doi.org/10.1016/j.inffus.2025.103257.

12. Dingle Robertson, L., McNairn, H., van der Kooij, M., Jiao, X., Ihuoma, S. & Joosse, P. "Monitoring autumn agriculture activities using Synthetic Aperture Radar (SAR) and coherence change detection". *Heliyon*. 2023; 9 (6): e17322. DOI: https://doi.org/10.1016/j.heliyon.2023.e17322.

13. Kılıç, D. K. & Nielsen, P. "Comparative analyses of unsupervised PCA K-means change detection algorithm from the viewpoint of follow-up plan". *Sensors*. 2022; 22 (23): 9172, https://www.scopus.com/pages/publications/85143518617. DOI: https://doi.org/10.3390/s22239172.

14. Liu, B., Chen, H., Li, K. & Yang, M. Y. "Transformer-based multimodal change detection with multitask consistency constraints". *Inf. Fusion*. 2024; 108: 102358, https://www.scopus.com/pages/publications/85188674553.
DOI: https://doi.org/10.1016/j.inffus.2024.102358.

15. Jiang, N., Li, P. & Feng, Z. "Detecting tropical freshly-opened swidden fields using a combined algorithm of continuous change detection and support vector machine". *International Journal of Applied Earth Observation and Geoinformation*. 2025; 136: 104403, https://www.scopus.com/pages/publications/85216902958. DOI: https://doi.org/10.1016/j.jag.2025.104403.

16. Kasahun, M. & Legesse, A. "Machine learning for urban land use/ cover mapping: Comparison of artificial neural network, random forest and support vector machine, a case study of Dilla town". *Heliyon*. 2024; 10 (20): e39146, https://www.scopus.com/pages/publications/85206327870. DOI: https://doi.org/10.1016/j.heliyon.2024.e39146.

17. Ji, S., Liu, K., Ling, B., Li, J., Wang, J. & Ma, X. "A study on improved random forest-based anomaly detection of regional tariff data under distributed photovoltaic access". *Results in Engineering*. 2025; 27: 105920, https://www.scopus.com/pages/publications/105009248358. DOI: https://doi.org/10.1016/j.rineng.2025.105920.

18. Londschien, M., Bühlmann, P. & Kovács, S. "Random Forests for Change Point Detection". *Journal of Machine Learning Research*. 2023; 23 (216): 1–45. DOI: https://doi.org/10.48550/arXiv.2205.04997.

19. Zhang, Z., Liu, S., Qin, Y. & Wang, H. "MATNet: Multilevel attention-based transformers for change detection in remote sensing images". *Image Vision Comput.* 2024; 151: 105294, https://www.scopus.com/pages/publications/85205551276. DOI: https://doi.org/10.1016/j.imavis.2024.105294.

20. Drabech, Z., Douimi, M. & Zemmouri, E. "A Markov random field model for change points detection". *Journal of Computational Science*. 2024; 83: 102429, https://www.scopus.com/pages/publications/85203427833. DOI: https://doi.org/10.1016/j.jocs.2024.102429.

21. Pushpalatha, V., Mallikarjuna, B., Mahendra, N., Subramoniam, S. R. & Swamy, M. "Land Use and Land Cover Classification for Change Detection Studies Using Convolutional Neural Network". *Applied Computing and Geosciences*. 2025; 25: 100227, https://www.scopus.com/pages/publications/85216592247. DOI: https://doi.org/10.1016/j.acags.2025.100227.

22. Sefrin, O., Riese, F. M. & Keller, S. "Deep learning for land cover change detection". *Remote Sens.* 2021; 13 (1): 78, https://www.scopus.com/pages/publications/85098560253. DOI: https://doi.org/10.3390/rs13010078.

23. Kashtan, V. Yu. & Hnatushenko, V. V. "Intelligent technology for land cover monitoring due to amber mining on optical satellite images". *Naukovyi Visnyk Natsionalnoho Hirnychoho Universytetu*. 2025; (3): 156–164, https://www.scopus.com/pages/publications/105015866441.
DOI: https://doi.org/10.33271/nvngu/2025-3/156.

24. Tariku, G., Ghiglieno, I., Simonetto, A., Gentilin, F., Armiraglio, S., Gilioli, G. & Serina, I. "Advanced image preprocessing and integrated modeling for UAV plant image classification". *Drones*. 2024; 8 (11): 645, https://www.scopus.com/pages/publications/85210246170?origin=resultslist. DOI: https://doi.org/10.3390/drones8110645.

25. Yuan, H. & Hu, W. "Image retrieval method based on data mining and deep residual network". Systems and Soft Computing. 2025; 7: 200331, https://www.scopus.com/pages/publications/105008518224. DOI: https://doi.org/10.1016/j.sasc.2025.200331.

26. Gianoli, A. "Unlocking patterns in urban land use efficiency: A global analysis using XGBoost and Bayesian networks". *Land Use Policy*. 2026; 160: 107838, https://www.scopus.com/pages/publications/105020725874.
DOI: https://doi.org/10.1016/j.landusepol.2025.107838.

27. "Aerial images". *Google Earth*. – Available from: https://earth.google.com. – [Accessed: Jan 30, 2026].

28. Deng, K., Hu, X., Zhang, Z., Su, B., Feng, C., Zhan, Y., Wang, X. & Duan, Y. "Cross-modal change detection using historical land use maps and current remote sensing images". *ISPRS J. Photogramm. Remote Sens.* 2024; 218: 114–132, https://www.scopus.com/pages/publications/85206975744. DOI: https://doi.org/10.1016/j.isprsjprs.2024.10.010.

**Conflicts of Interest:** The authors declare that they have no conflict of interest regarding this study, including financial, personal, authorship, or other, which could influence the research and its results presented in this article

Received 29.01.2026
Received after revision 12.03.2026
Accepted 17.03.2026

**DOI: https://doi.org/10.15276/hait.09.2026.14**
**УДК 004.056:621.391**

# Методологія розпізнавання змін земного покриву на аерофотознімках із використанням глибокої згорткової нейронної мережі та ансамблевого алгоритму градієнтного підсилення

**Каштан Віта Юріївна**[1)]
ORCID: https://orcid.org/0000-0002-0395-5895; kashtan.v.yu@nmu.one. Scopus Author ID: 57201902879
**Гнатушенко Володимир Володимирович**[1)]
ORCID: https://orcid.org/0000-0003-3140-3788; vvgnat@ukr.net. Scopus Author ID: 6505609275
[1)] Національний технічний університет «Дніпровська політехніка», пр. Дмитра Яворницького, 19. Дніпро, 49005, Україна

## АНОТАЦІЯ

Задачі моніторингу змін земного покриву за аерофотознімками високого просторового розрізнення ускладнюються високою просторовою деталізацією сцен, спектральною неоднорідністю поверхні та наявністю візуально подібних антропогенних об’єктів. Особливо складною є ідентифікація зон видобутку бурштину, які характеризуються просторово розірваною морфологічною структурою, наявністю множинних локальних порушень різного розміру та форми, а також високою внутрішньою просторовою неоднорідністю, що істотно обмежує ефективність класичних попіксельних і порогових методів. **Метою роботи є розробка** методології автоматизованого розпізнавання змін земного покриву за аерофотознімками високого просторового розрізнення, що ґрунтується на використанні згорткової нейронної мережі для вилучення високорівневих просторово-текстурних ознак та алгоритмів градієнтного бустингу для подальшої класифікації виявлених змін. **Методологія** реалізує багатоступеневу схему обробки даних, що включає підготовку та ручне анотування аерофотознімків, формування навчальних і тестових вибірок, вилучення ознак на рівні локальних фрагментів зображення, класифікацію змін і просторову агрегацію результатів patch-рівня з формуванням безперервної тематичної карти. На відміну від традиційних підходів, запропоноване рішення забезпечує урахування просторового контексту та текстурної організації поверхні, а також дозволяє відокремлювати зони видобутку бурштину від інших антропогенних змін, що є критично складною задачею для аерофотознімків високого просторового розрізнення. Реалізація та тестування запропонованої методології виконувалися у середовищі Python із використанням бібліотек TensorFlow та Keras для побудови та навчання згорткової нейронної мережі, а також бібліотеки градієнтного підсилення для реалізації ансамблевого градієнтного класифікатора. У результаті застосування методології сформовано карту змін земного покриву за трьома семантичними класами: «без змін», «зони видобутку бурштину» та «інші зміни», а також отримано класифіковану карту з векторизованими контурами порушених ділянок. Кількісна оцінка з використанням гармонійного середнього значення точності та відтворення, коефіцієнта перетину над об'єднанням, середньоквадратичної похибки, середньої абсолютної похибки та нормалізованої крос-кореляції з нульовим середнім значенням продемонструвала вищу ефективність у виявленні видобутку бурштину, перевершивши стандартні моделі нейронних мереж. **Практичне значення** запропонованої методології полягає у можливості її використання для автоматизованого моніторингу антропогенних порушень, оцінки площ деградації ландшафтів, підтримки екологічного контролю та прийняття управлінських рішень у сфері природокористування.

**Ключові слова:** аерофотознімки; зміни земногго покриву; глибока згорткова мережа; градієнтне підсилення; машинне навчання

## ABOUT THE AUTHORS

**Vita Yu. Kashtan** - Candidate of Engineering Sciences, Associate Professor, Information Technology and Computer Engineering Department. Dnipro University of Technology. 19, Dmytro Yavornytskoho Ave, Dnipro, 49005, Ukraine
ORCID: https://orcid.org/https://orcid.org/ 0000-0002-0395-5895; kashtan.v.yu@nmu.one. Scopus Author ID: 57201902879
***Research field*:** Machine Learning; Data Science; Data Preprocessing; Analysis of Aerospace Images; Image Detection

**Каштан Віта Юріївна** - кандидат технічних наук, доцент, доцент кафедри Інформаційних технологій та комп'ютерної інженерії. Національний технічний університет «Дніпровська політехніка», пр. Дмитра Яворницького, 19. Дніпро, 49005, Україна

**Volodymyr V. Hnatushenko** - Doctor of Engineering Sciences, Professor, Head of Information Technology and Computer Engineering Department. Dnipro University of Technology. 19, Dmytro Yavornytskoho Ave, Dnipro, 49005, Ukraine
ORCID: https://orcid.org/0000-0003-3140-3788; vvgnat@ukr.net
***Research field*:** Machine Learning; Data Science; Data Preprocessing; Analysis of Aerospace Images; Image Recognition

**Гнатушенко Володимир Володимирович** - доктор технічних наук, професор, завідувач кафедри Інформаційних технологій та комп'ютерної інженерії. Національний технічний університет «Дніпровська політехніка», пр. Дмитра Яворницького, 19. Дніпро, 49005, Україна